7-1-2013

Alternative Ear-Canal Measures Related to Absorbance

S. T. Neely
Boys Town National Research Hospital

S. Stenfelt
Boys Town National Research Hospital

Kim S. Schairer
East Tennessee State University, schairer@etsu.edu

Citation Information

Neely, S. T.; Stenfelt, S.; and Schairer, Kim S.. 2013. Alternative Ear-Canal Measures Related to Absorbance. *Ear and Hearing*. Vol.34 Suppl 1 72S-77S. https://doi.org/10.1097/AUD.0b013e31829c7229
ISSN: 0196-0202

Alternative Ear-Canal Measures Related to Absorbance

Published in final edited form as:
Ear Hear. 2013 July ; 34(7 0 1): 72s–77s. doi:10.1097/AUD.0b013e31829c7229.

Alternative Ear-Canal Measures Related to Absorbance

Stephen T. Neely[1], **Stefan Stenfelt**[2], and **Kim S. Schairer**[3]

[1]Boys Town National Research Hospital, 555 North 30th Street, Omaha, Nebraska 68131

[2]Department of Clinical and Experimental Medicine, Linköping University, Linköping Sweden

[3]James H. Quillen Veteran's Administration Medical Center, Mountain Home, TN 37684

Abstract

Several alternative ear-canal measures are similar to absorbance in their requirement for prior determination of a Thévenin-equivalent sound source. Examples are (1) sound intensity level (SIL), (2) forward-pressure level (FPL), (3) time-domain ear-canal reflectance (TDR), and (4) cochlear reflectance (CR). These four related measures are similar to absorbance in their utilization of wide-band stimuli and their focus on recording ear-canal sound pressure. The related measures differ from absorbance in how the ear-canal pressure is analyzed and in the type of information that is extracted from the recorded response. SIL and FPL have both been shown to be better as measures of sound level in the ear canal compared to sound pressure level (SPL) because they reduced calibration errors due to standing waves in studies of behavioral thresholds and otoacoustic emissions. TDR may be used to estimate ear-canal geometry and may have the potential to assess middle-ear pathology. CR reveals information about the inner ear that is similar to what is provided by other types of otoacoustic emissions and may have theoretical advantages that strengthen its interpretation.

INTRODUCTION

Wideband acoustic immittance studies often focus on measurements of absorbance and power reflectance. The purpose of this paper is to describe four related measurements and their potential benefits for clinical application, which include improved in-the-ear sound calibration, improved ear-canal volume estimates, and information about inner-ear function. The definitions of these alternative measurements, which are presented in this section, will reveal how they are related to absorbance.

Absorbance describes the proportion of sound power absorbed from a sound source by a waveguide (such as the ear canal) and is the complement of *power reflectance* (*e.g.*, Rosowski, this supplement). Power reflectance is the squared magnitude of *pressure reflectance,* which we simply call *reflectance*. Reflectance allows the pressure measured at the entrance to a waveguide to be separated into forward-propagating and reverse-propagating components. This separation is essential to the calculation of absorbed power and to the calculation of other measures of sound in the ear canal.

Reflectance at the termination (x=0) of an air-filled measurement tube depends on the *termination impedance* $Z_T(f, 0)$ and *characteristic impedance* of the tube Z_o (Rosowski, this supplement):

Corresponding Author: Stephen T. Neely, Boys Town National Research Hospital, 555 North 30th Street, Omaha, NE 68131, Telephone: 402-498-6751, Stephen.Neely@boystown.org.

$$\mathbf{R}=\frac{Z_T-Z_o}{Z_T+Z_o}. \quad (1)$$

In this paper, we generalize this definition of reflectance by equating the characteristic impedance Z_o with the *surge impedance*. Theoretically, the surge impedance is the real part of $Z_T(f, 0)$ in the high-frequency limit as $f\rightarrow\infty$. The advantage of the surge impedance (over calculations of characteristic impedance based on cross-sectional area) is that it can be estimated numerically for any arbitrary termination impedance, even when the cross-sectional area is unknown (*e.g.*, Rasetshwane and Neely, 2011).

Calibration of sound levels in the ear canal is problematic because (1) ear-canal geometry varies widely across individual ears and (2) much of sound delivered to the ear is reflected at the eardrum. The variation of ear-canal length and volume makes pressure calibrated in a standard volume an inaccurate predictor of the sound power delivered to the ear. Reflection of sound at the eardrum causes alternating regions of pressure cancellation and enhancement depending on the relative phase of the forward-propagating and reverse-propagating pressure-wave components that combine to produce the total pressure measured by a microphone in the ear canal. This makes the total pressure an inaccurate predictor of sound power delivered to the ear. The constructive and destructive interaction between pressure-wave components is sometimes described as a *standing-wave* effect (*e.g.*, Siegel, 1994). Reflectance improves predictions of sound power delivered to the ear by allowing a method of separation of the forward-propagating and reverse-propagating components. This is equivalent to saying that the termination impedance allows absorbed power to be estimated from measured pressure.

Keefe *et al.* (1993) defined "power input to the ear" or *absorbed power* as

$$\mathbf{P}=\frac{1}{2}G_T\left|P_T\right|^2, \quad (2)$$

where $P_T(f, 0)$ is the measured pressure at x=0 and G_T is the real part of the termination admittance: $G_T=\Re[1/Z_T]$.

Neely and Gorga (1998) suggested the use of sound intensity level (SIL) as a measure of sound level in the ear canal. They defined SIL as the decibel equivalent of acoustic intensity, which is defined as absorbed power per unit area:

$$\mathrm{SIL}=10\cdot\log_{10}\left(\frac{1}{2}G_T\left|P_T\right|^2\right). \quad (3)$$

They showed that behavioral thresholds measured in terms of SIL were much less sensitive to variations in "probe-insertion depth" compared to sound pressure level (SPL) measured by a microphone in the ear canal. The "probe" is a combination of microphone and sound source designed for measurement of otoacoustic emissions.

There remains uncertainty about whether the inner ear is better characterized as a *power detector* or a *pressure detector* (*e.g.*, Puria *et al.*, 1997). If the ear is more like a pressure detector, then forward-pressure level (FPL) might be a better measure of sound level in the ear-canal. Scheperle *et al.* (2008) compared both SIL and FPL with SPL (*i.e.*, pressure at the microphone) as measures of stimulus levels for distortion-product otoacoustic emissions

(DPOAE) recordings. Standing-wave effects were known to be a problem for DPOAE measurements due to reliance on in-the-ear sound-level calibration (*e.g.*, Siegel and Hirohata, 1994). Scheperle *et al.* defined forward pressure as

$$P_f = \frac{1}{2}\left(1 + \frac{Z_o}{Z_T}\right) P_T, \quad (4)$$

so that

$$\mathrm{FPL} = 20 \cdot \log_{10}\left(\frac{1}{2}\left|1 + Z_0/Z_T\right| \cdot \left|P_T\right|\right). \quad (5)$$

Note that this definition of forward pressure is consistent with the interpretation that the termination pressure $P_T(f, 0)$ is the sum of the forward pressure $P_f(f, 0)$ and reflected pressure $P_r(f, 0)$, defined as

$$P_r = \frac{1}{2}\left(1 - \frac{Z_o}{Z_T}\right) P_T. \quad (6)$$

Also, note that these definitions of P_f and P_r are consistent with the interpretation of reflectance as being the ratio of reflected pressure to forward pressure.

$$\mathbf{R} = \frac{P_r}{P_f}. \quad (7)$$

Scheperle *et al.* compared how SIL and FPL differed from SPL with respect to the sensitivity of recorded DPOAE levels when the probe-insertion depth was deliberately changed. The results of their study are described in the next section.

Rasetshwane and Neely (2011) described the use of ear-canal reflectance to estimate the cross-sectional area as a function of distance from the probe to the eardrum. Their method involves transforming reflectance, which is usually represented as a function of frequency, into a real-valued function of time. A solution to the inverse problem (*i.e.*, the problem of determining cross-sectional area from reflectance) that had previously been applied only to theoretical representations of acoustic horns was shown to produce reasonable estimates of ear-canal profiles from time-domain reflectance (TDR) measurements.

Ear-canal contributions to TDR occur within about 0.3 ms, whereas cochlear contributions to TDR occur after 1 ms. Rasetshwane and Neely (2012) described time-frequency analyses of the cochlear contribution to ear-canal reflectance. They showed that *cochlear reflectance* (CR) occurs within a frequency-dependent time range that is consistent with other cochlear-response measures. CR level dependence is similar to what has been observed in measurements of otoacoustic emissions and tone-burst evoked auditory brainstem responses.

ALTERNATIVE MEASURES

Similar methods are shared by the four studies (Neely and Gorga, 1998; Scheperle *et al.*, 2008; Rasetshwane and Neely, 2011; and Rasetshwane and Neely, 2012) that were cited above as having introduced the four alternative measurements (SIL, FPL, TDR, and CR). These methods are summarized briefly below and selected highlights of the results are

described. The focus is on results that have relevance for clinical applications. Further details are available in the original publications.

Sound Intensity Level

Methods—Neely and Gorga (1998) used an ER-10C probe microphone (Etymōtic Research, Elk Grove Village, IL) both to deliver stimuli to the ear canal and to record sound pressure at the plane of the probe. Stimuli were generated with a 16-bit sound card (Tahiti, Turtle Beach, Valhalla, NY) at a sampling rate of 44.1-kHz. Custom software (PUTT, Neely and Liu, 1994) was used to control the stimulus generation and measure behavioral thresholds. Prior to measurement of thresholds in human subjects, the Thévenin-equivalent source impedance and source pressure were determined by methods similar to those suggested by Allen (1986), Keefe *et al.* (1992), and Voss and Allen (1994). Behavioral thresholds to tonal stimuli were measured in 75 normal-hearing subjects at 12 frequencies for two probe-insertion depths. Five of the frequencies were standard audiometric frequencies (0.5, 1, 2, 4, 8 kHz). Seven additional frequencies were distributed near the standing-wave notch frequency at ¼-octave intervals. The first probe insertion was as deep as possible. A second set of measurements was made after reducing the probe-insertion depth until the notch frequency decreased (or increased) by about ½ octave. (Data from seven subjects were excluded from further analysis because the notch frequency shifted less than ¼ octave.) The response measure of interest in this study was the change in behavioral threshold between the two probe-insertion depths.

Results—The main result of the Neely and Gorga (1998) study was elimination of the behavioral-threshold sensitivity to probe-insertion depth when the sound level in the ear-canal was expressed in terms of SIL instead of SPL. This result is seen in the left panel of Fig. 1 by comparing the open circle (SPL) to the filled circle (SIL) at the notch frequency (of the first probe insertion), which is located at 0 on the x axis. The average change in threshold between the two probe insertions at the notch frequency was 11 dB when stimulus levels were specified in SPL and was reduced to nearly 0 dB when specified in SIL. The threshold change for SIL was consistently near 0 dB at all 12 test frequencies. Voltage delivered to the probe was the third reference measure for which results are shown in Fig. 1. Voltage calibration was less sensitive to probe shifts than SPL because it does not depend on any measurement in the ear canal, so it is not susceptible to standing-wave effects. However, voltage calibration is less accurate than SIL because it is affected by changes in ear-canal impedance, which is known to vary widely across individual ears.

Discussion—SIL, which is the decibel equivalent of *absorbed power per unit area*, was shown to eliminate the standing-wave effects on behavioral thresholds that have been observed when using in-the-ear SPL calibration (Neely and Gorga, 1998). More recent studies (McCreery *et al.*, 2009; Lewis *et al.*, 2009) have demonstrated similar elimination of standing-wave effects on behavioral thresholds with sound delivered through the sound-port of custom-fit earmolds.

Forward Pressure Level

Methods—Scheperle *et al.* (2008) used an ER-10C probe microphone with a 24-bit sound card (CardDeluxe, Digital Audio Labs, Chanhassen, MN) at a sampling rate of 32 kHz. They used custom software (EMAV, Neely and Liu, 1994) to produce two simultaneous tones f_1 and f_2 on separate sound sources and record DPOAEs from 21 normal-hearing human subjects at 13 f_2 frequencies, 5 L_2 levels, and two probe-insertion depths. Stimulus levels were specified three different ways (SPL, SIL, or FPL) with $L_1 = +\ 39\ 0.4L_2$ (Kummer *et al.*, 1998). The second probe insertion was about 2–3 mm less deep than the

first insertion. The response measure of interest in this study was the change in DPOAE level between the two probe insertions.

Results—As with the Neely and Gorga (1998) study, probe-insertion depth was manipulated by Scheperle *et al.* (2008), but their response measure was DPOAE level instead of behavioral threshold. Their results (shown in Fig. 2) demonstrate a similar reduction in sensitivity to probe-insertion depth when stimuli were specified in SIL or FPL instead of SPL. In this study, FPL gave about the same benefit as SIL; however, the fact that neither SIL nor FPL completely eliminated probe-shift sensitivity was thought to indicate a need for further improvements in the methods used to determine the Thévenin-equivalent source characteristics.

Discussion—Scheperle *et al.* (2008) showed that SIL and FPL were about equally effective at removing the sensitivity of DPOAE levels to deliberate changes in probe-insertion depth compared to when stimulus levels were specified in SPL. In contrast (and contrary to expectations), a subsequent study of DPOAE in a hearing-screening paradigm (*i.e.*, classifying subjects as either normal-hearing or hearing-impaired) failed to demonstrate significant improvement in test performance when stimulus levels are specified as FPL instead of SPL (Burke *et al.*, 2010). A more recent DPOAE study (Kirby *et al.*, 2011) appears to show some test-performance benefit with FPL; however, the excellent test performance obtained even when using SPL restricts the possible range for seeing additional improvements. In summary, the results of these studies do not provide compelling evidence that FPL is significantly better than SPL in a DPOAE hearing-screening paradigm. Apparently, group-based assessments of test performance are relatively insensitive to stimulus-level errors (due to standing-wave effects) because these errors are large in only a few ears, so the pass/fail decision is seldom affected. However, the FPL advantage is still clearly observed in the few ears where standing-wave effects are large.

Keefe and Schairer (2011) observed that when stimulus-frequency otoacoustic emissions (SFOAE) tuning curves are measured with stimulus levels defined in terms of absorbed power level (APL) instead of SPL, the agreement at 8 kHz between the measured tuning and the predictions of cochlear tuning by Shera *et al.* (2010) based on SFOAE latency was improved. Keefe and Schairer suggested that APL calibration may also be useful in other auditory measures.

Souza *et al.* (2010) tested several different measures of sound level in the ear canal, including SIL and FPL, to determine which measure gave the least behavioral-threshold sensitivity to changes in probe-insertion depth. FPL thresholds were significantly less sensitive to probe shifts than SIL thresholds. Their results suggest that FPL describes the quantity of sound that is detected by the ear better than SIL. In other words, the inner ear is more similar to a pressure detector than a power detector, which is consistent with the observations of Puria *et al.* (1997).

Time-Domain Reflectance

Methods—Rasetshwane and Neely (2011) used an ER-10B+ probe microphone (Etymōtic Research, Elk Grove Village, IL) with a modified-tweeter sound source (TW010F1, Audax, France) and a 24-bit sound card (Layla3G, Echo, Santa Barbara, CA) at a sampling rate of 48 kHz. (A power amplifier reduced the electrical load of the tweeter on the sound-card output.) They used custom software (EMAV) to deliver chirp stimuli and record wideband ear-canal sound pressure from 24 human subjects. Reflectance was calculated in the frequency domain by using the surge component of the termination impedance to represent Z_0 in Eq. (1). The corresponding TDR was computed by applying a Blackman window to

the frequency-domain reflectance and taking an inverse Fourier transform. (Application of a window in the frequency domain reduced "ringing" artifacts in the time domain.) The response measure of primary interest in this study was the ear-canal contribution to TDR, which was observed to occur in the time range 0 to 0.2 ms. Ear-canal TDR allowed estimation of individual ear-canal profiles (*i.e.*, area as a function of distance from the eardrum) by using the inverse-solution method described by Rasetshwane *et al*. (2012).

Results—The mean and inter-quartile range of the reflectance magnitude as a function of frequency (Rasetshwane and Neely, 2011) are shown in the upper panel of Fig. 3. The corresponding *delay*, which is computed from the phase of the reflectance, is shown in the lower panel. The TDR data shown in Fig. 4 was computed as the inverse Fourier transform of the frequency-domain reflectance shown in Fig. 3. A time-shift correction was applied to individual TDR waveforms to align all of the major peaks at t=0.14 ms, which was the average time that this peak occurred in individual TDRs. An inverse solution (Rasetshwane *et al*., 2012) was applied to the TDR to estimate the ear-canal area as a function of distance from the eardrum. Figure 5 compares mean and inter-quartile range of the area functions derived from TDR with ear-canal areas from the extant literature obtained by other measurement methods. The TDR-based areas are similar, although perhaps slightly smaller than other area measurements, which were made in cadaveric ears.

One reason that the TDR-based areas are smaller than other estimates is that the TDR measurement is only possible between the plane of the probe and the eardrum. TDR measurements more than 10 mm from eardrum are only possible in relatively long ear-canals. Thus, as distance from the eardrum increases, relatively short ear-canals are increasingly under-represented in the group-averaged area estimates shown in Fig. 5.

Discussion—The time-shift that aligns TDR peaks appears to reduce variability due to differing distance between the probe and eardrum across individual ears. This reduction in variability can be appreciated visually by observing that the shaded region is smaller in Fig. 4 compared to Fig. 3. The peak alignment is only possible because reflectance, unlike absorbance, retains phase information. This method of potentially reducing the variability in ear-canal reflectance by TDR peak alignment demonstrates another possible advantage of reflectance measurements over power reflectance or absorbance measurements.

Cochlear Reflectance

Methods—Rasetshwane and Neely (2012) used the same measurement system and response analysis described above to obtain ear-canal TDR in response to both chirp and broad-band noise (BBN) stimuli. A high-level chirp TDR was subtracted from lower-level BBN TDRs to remove measurement-system artifacts. The response measure of primary interest in this study was the cochlear contribution to the residual TDR, which was observed to occur in the time range of 1–30 ms. A time-dependent frequency range was specified to further limit the time-frequency region that contributed to estimates of CR magnitude. This frequency range at any particular time was defined as the set of frequencies having more than 4 cycles and less than 40 cycles. These limits correspond to diagonal lines on a time-frequency plot along which the product of time and frequency equals the specified number of cycles.

Results—An example of ear-canal TDR from a typical subject is shown in Fig. 6 over the time range from 0 to 30 ms. Each waveform represents a different stimulus level, which is indicated on the y axis. These waveforms represent TDR responses to BBN stimuli after subtracting a chirp TDR to remove measurement-system artifacts. The ear-canal and middle-ear contributions to TDR occur within the first millisecond so are not easily seen in Fig. 6.

The cochlear contribution to TDR, which we call CR, occurs mainly in the time range of 1–30 ms. CR is largest at the lowest stimulus level and its magnitude decreases as stimulus level increases.

Figure 7 shows a time-frequency analysis of the lowest level TDR from Fig. 6. Note that the frequency content of the TDR appears to shift lower with increasing time, which is consistent with reflection that originates from the more apical region of the basilar membrane. The CR appears to be bounded by the lower and upper dashed curves superimposed on the spectrogram, which represent 4 and 40 cycles, respectively.

Discussion—CR is a type of otoacoustic emission, so has many features in common with other types of otoacoustic emissions (OAEs). As with SFOAEs, CR is thought to be generated primarily by coherent reflection (*e.g.*, Shera and Guinan, 1999). An advantage of CR over SFOAEs is reduced dependence on ear-canal acoustics due to deconvolution by the forward pressure.

CONCLUSIONS

Absorbed power level (or SIL) is a better measure of sound level in the ear canal than SPL because it eliminates calibration errors due to standing-wave effects. FPL also eliminates standing-wave effects and may be preferable to SIL because behavioral thresholds measured in FPL are less sensitive to probe shifts. Reflectance provides more information about the ear-canal than power reflectance or absorbance because it retains phase information as well as the magnitude information. The additional information that reflectance phase provides a potential method of reducing some of the variability in ear-canal reflectance measurements by time-shift alignment of TDR peaks. Another potential advantage that reflectance may offer is more efficient extraction of the cochlear contribution (*i.e.*, CR) by means of targeted time-frequency analysis.

Acknowledgments

Work on this review was supported by the NIH grant R01 DC8318 to the first author. Contributions of the co-authors of the four reviewed studies (Michael Gorga, Rachel Scheperle, Judy Kopun, and Daniel Rasetshwane) are gratefully acknowledged. Some of the apparatus used to measure reflectance was generously provided by Jon Siegel at Northwestern University.

References

Allen, JB. Measurement of Eardrum Acoustic Impedance. In: Allen, JB.; Hall, JL.; Hubbard, A., et al., editors. Peripheral Auditory Mechanisms. New York: Springer-Verlag; 1986. p. 44-51.

Burke SR, Rogers AR, Neely ST, et al. Influence of calibration method on DPOAE measurements: I. Test performance. Ear Hear. 2010; 31:533–545. [PubMed: 20458246]

Egolf DP, Nelson DK, Howell HC III, Larson VD. Quantifying ear canal geometry with multiple computer-assisted tomographic scans. J Acoust Soc Am. 1993; 93:2809–2819. [PubMed: 8315148]

Johansen PA. Measurement of the human ear canal. Acustica. 1975; 33:349–351.

Keefe DH, Ling R, Bulen JC. Method to measure acoustic impedance and reflection coefficient. J Acoust Soc Am. 1992; 91:470–485. [PubMed: 1737890]

Keefe DH, Schairer KS. Specification of absorbed-sound power in the ear canal: Application to suppression of stimulus frequency otoacoustic emissions. J Acoust Soc Am. 2011; 129:779–791. [PubMed: 21361437]

Keefe DH, Bulen JC, Hoberg K, Burns EM. Ear-canal impedance and reflection coefficient of human infants and adults. J Acoust Soc Am. 1993; 94:2617– 2638. [PubMed: 8270739]

Kirby BJ, Kopun JG, Tan H, Neely ST, Gorga MP. Do “optimal” conditions improve distortion product otoacoustic emission test performance? Ear and Hearing. 2011; 32:230–237. [PubMed: 21057318]

Kummer P, Janssen T, Arnold W. The level and growth behavior of the 2f1-f2 distortion product otoacoustic emission and its relationship to auditory sensitivity in normal hearing and cochlear hearing loss. J Acoust Soc Am. 1998; 103:3431–3444. [PubMed: 9637030]

Lewis JD, McCreery RW, Neely ST, Stelmachowicz PG. Comparison of in-situ calibration methods for quantifying input to the middle ear. J Acoust Soc Am. 2009; 126(6):3114–3124. [PubMed: 20000925]

McCreery RW, Pittman AL, Lewis JD, Neely ST, Stelmachowicz PG. Use of forward pressure level (FPL) to minimize the influence of acoustic standing waves during probe-microphone measurements. J Acoust Soc Am. 2009; 126:15–24. [PubMed: 19603858]

Neely ST, Gorga MP. Comparison between intensity and pressure as measures of sound level in the ear canal. J Acoust Soc Am. 1998; 104:2925–2934. [PubMed: 9821338]

Neely, ST.; Liu, Z. Technical Memo No 17. Boys Town Research Hospital; Omaha, NE: 1994. EMAV: Otoacoustic emission averager.

Puria S, Peake WT, Rosowski JJ. Sound-pressure measurements in the cochlear vestibule of human-cadaver ears. J Acoust Soc Am. 1997; 101:2754–2770. [PubMed: 9165730]

Rasetshwane DM, Neely ST. Inverse solution of ear-canal area function from reflectance. J Acoust Soc Am. 2011; 130:3873–3881. [PubMed: 22225043]

Rasetshwane DM, Neely ST. Measurements of Wide-Band Cochlear Reflectance in Humans. J Assoc Res Otolaryngol. 2012; 13:591–607. [PubMed: 22688355]

Rasetshwane DM, Neely ST, Allen JB, Shera CA. Reflectance of acoustic horns and solution of the inverse problem. J Acoust Soc Am. 2012; 131:1863–1873. [PubMed: 22423684]

Scheperle RA, Neely ST, Kopun JG, Gorga MP. Influence of *in situ*, sound-level calibration on distortion-product otoacoustic emission variability. J Acoust Soc Am. 2008; 124:288–300. [PubMed: 18646977]

Shera CA, Guinan JJ Jr. Evoked otoacoustic emissions arise by two fundamentally different mechanisms: a taxonomy for mammalian OAEs. J Acoust Soc Am. 1999; 105:782–798. [PubMed: 9972564]

Shera CA, Guinan JJ Jr, Oxenham AJ. Otoacoustic estimation of cochlear tuning: Validation in the chinchilla. J Assoc Res Otolaryngol. 2010; 11:343–365. [PubMed: 20440634]

Siegel JH. Ear-canal standing waves and high-frequency sound calibration using otoacoustic emission probes. J Acoust Soc Am. 1994; 95:2589–2597.

Siegel JH, Hirohata ET. Sound calibration and distortion product otoacoustic emissions at high frequencies. Hearing Research. 1994; 80:146–152. [PubMed: 7896573]

Souza N, Dhar S, Siegel J. A Critical Test of Alternate Stimulus Level Measures for the Human Ear. Presented at the 33rd Annual MidWinter Meeting of the Assoc Res Otolryngol. 2010

Stinson MR, Lawton BW. Specification of the geometry of the human ear canal for the prediction of sound-pressure level distribution. J Acoust Soc Am. 1989; 85:2492–2503. [PubMed: 2745874]

Voss SE, Allen JB. Measurement of acoustic impedance and reflectance in the human ear canal. J Acoust Soc Am. 1994; 95:372–384. [PubMed: 8120248]

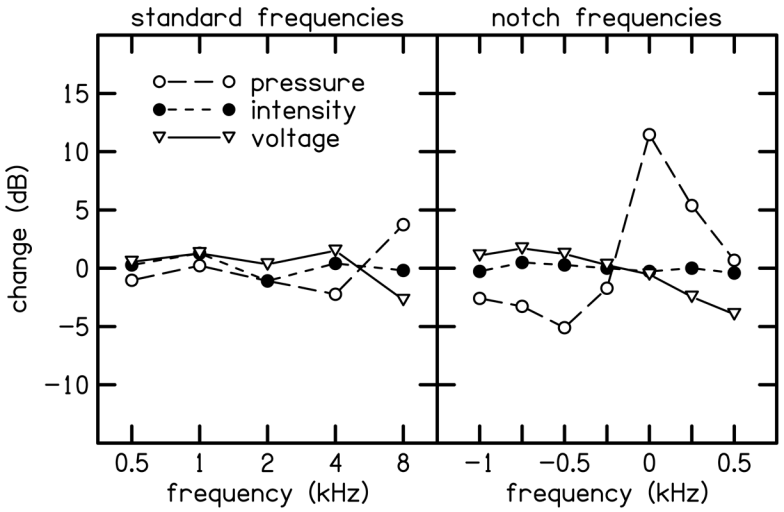

Figure 1.

SPL, SIL, and voltage threshold changes due to change of insertion depth. The open circles represent the mean change in SPL threshold, the filled circles represent the mean change in SIL threshold, and the triangles represent the change in voltage (dBV) to the probe at threshold. The 5 standard frequencies are shown in the left panel. The 7 additional frequencies near the notch frequency are shown in the right panel. Reprinted with permission from Neely, S. T., & Gorga, M.P., Journal of the Acoustical Society of America, 104, 2925–2934. Copyright (1998), Acoustical Society of America.

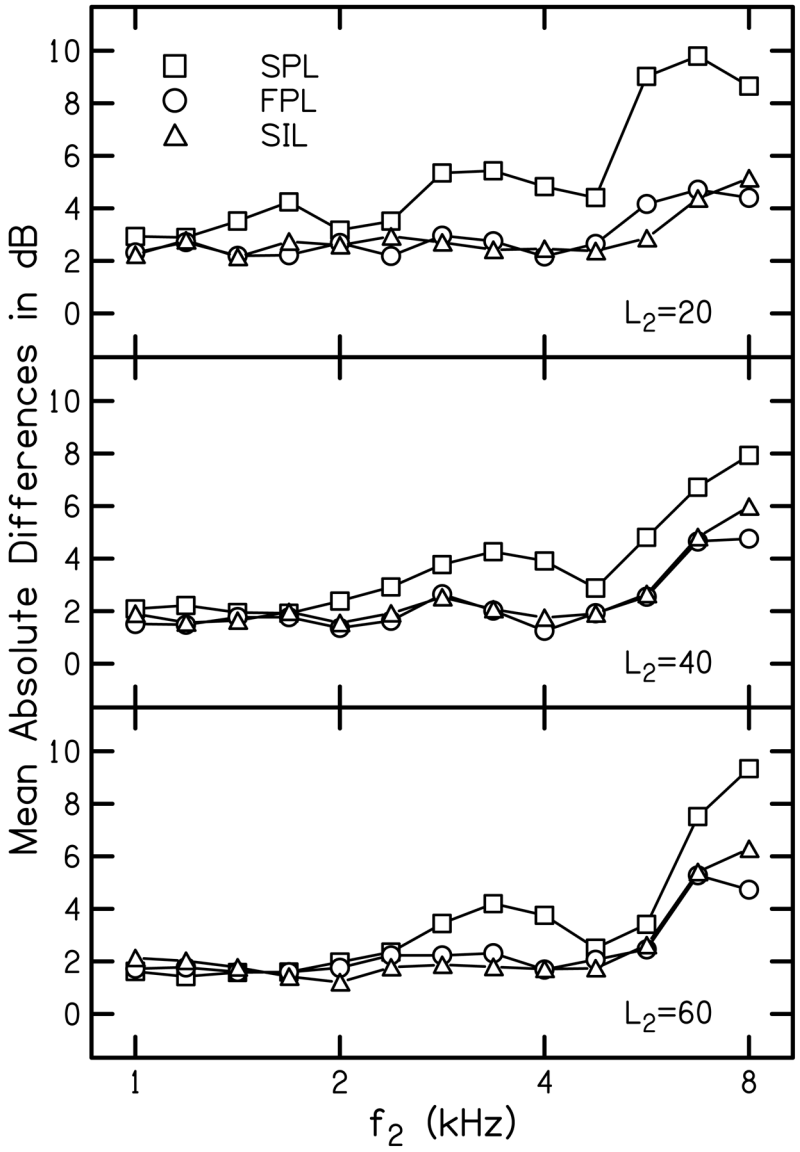

Figure 2.

DPgrams of the mean absolute changes in DPOAE levels due to changes in insertion depth (after individually correcting for the expected change due to other factors). The three calibration methods (SPL, FPL, and SIL) are compared for three L_2 levels (20, 40, and 60 dB). Reprinted with permission from Scheperle, R.A., et al., Journal of the Acoustical Society of America, 124, 288–300. Copyright (2008), Acoustical Society of America.

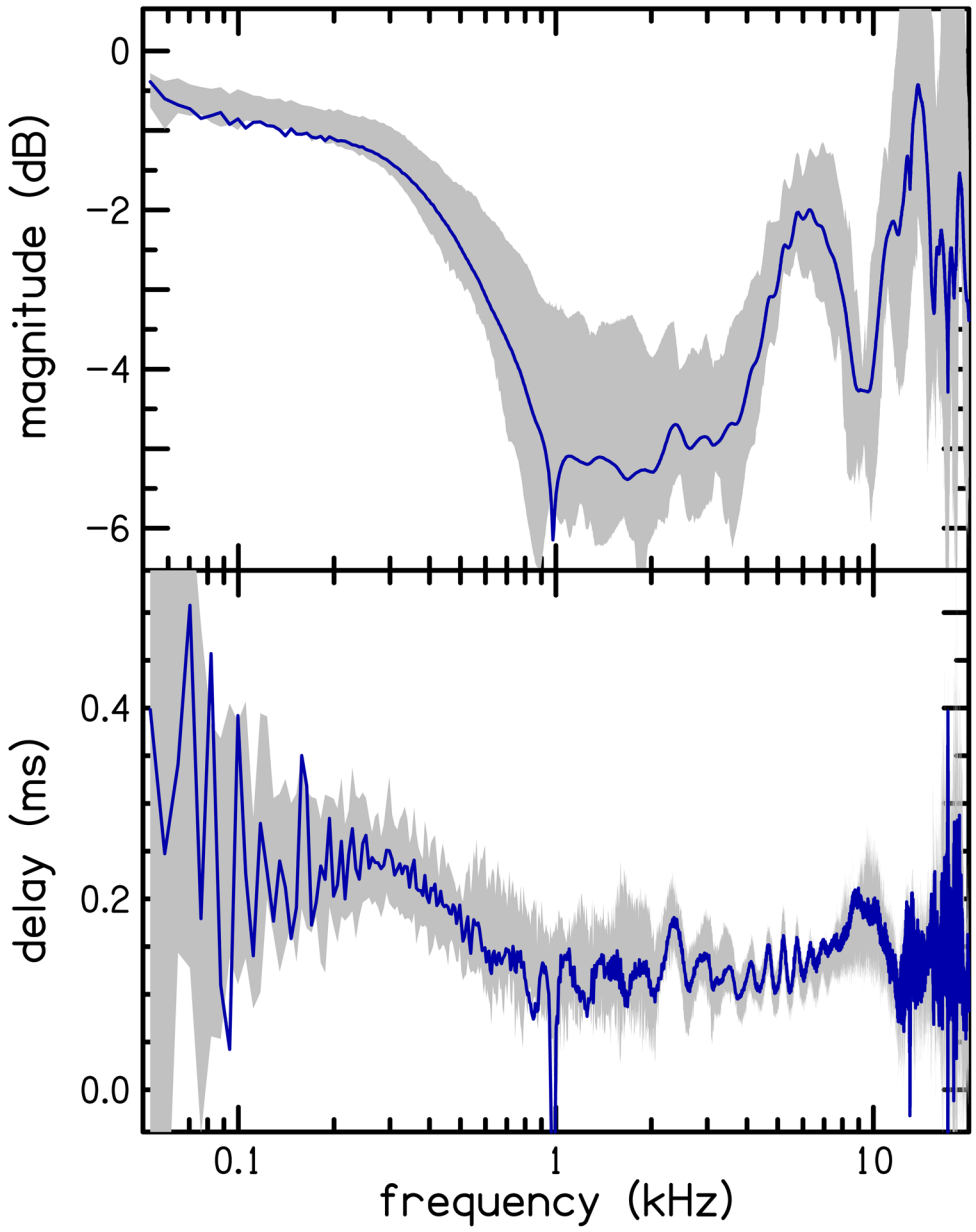

Figure 3.
Mean ear-canal frequency-domain reflectance. The shaded region indicates data between the 25th and 75th percentiles. Reprinted with permission from Rasetshwane D.M. & Neely S. T., Journal of the Acoustical Society of America, 130, 3873–3881. Copyright (2011). Acoustical Society of America.

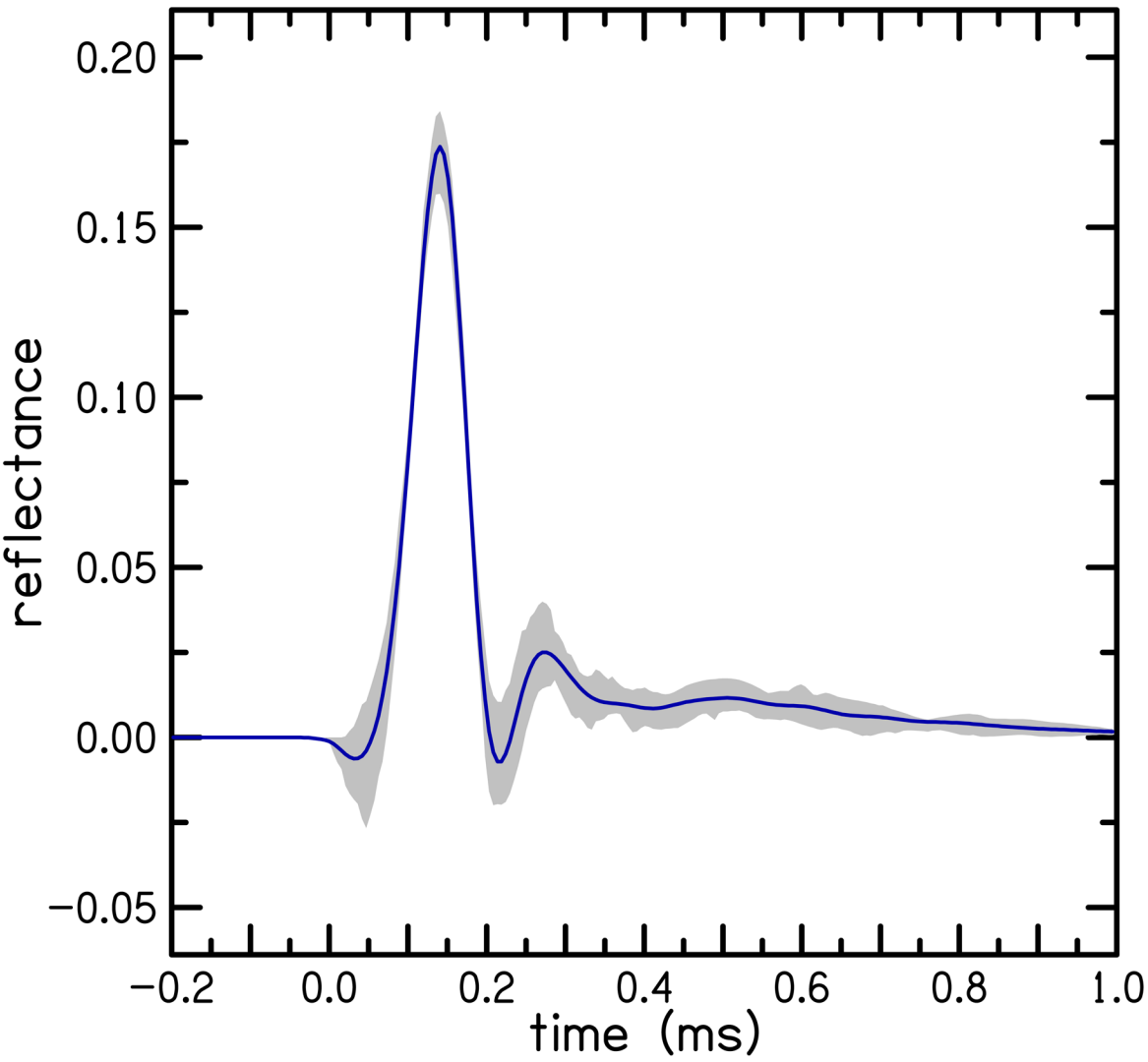

Figure 4.
Mean ear-canal time-domain reflectances (TDR). The TDR of individual subjects were translated in time so that the latency of the largest peak equals the average latency (0.14 ms). Shaded region indicates data between 25th and 75th percentiles. Reprinted with permission from Rasetshwane D.M. & Neely, S.T., Journal of the Acoustical Society of America, 130, 3873–3881. Copyright (2011). Acoustical Society of America.

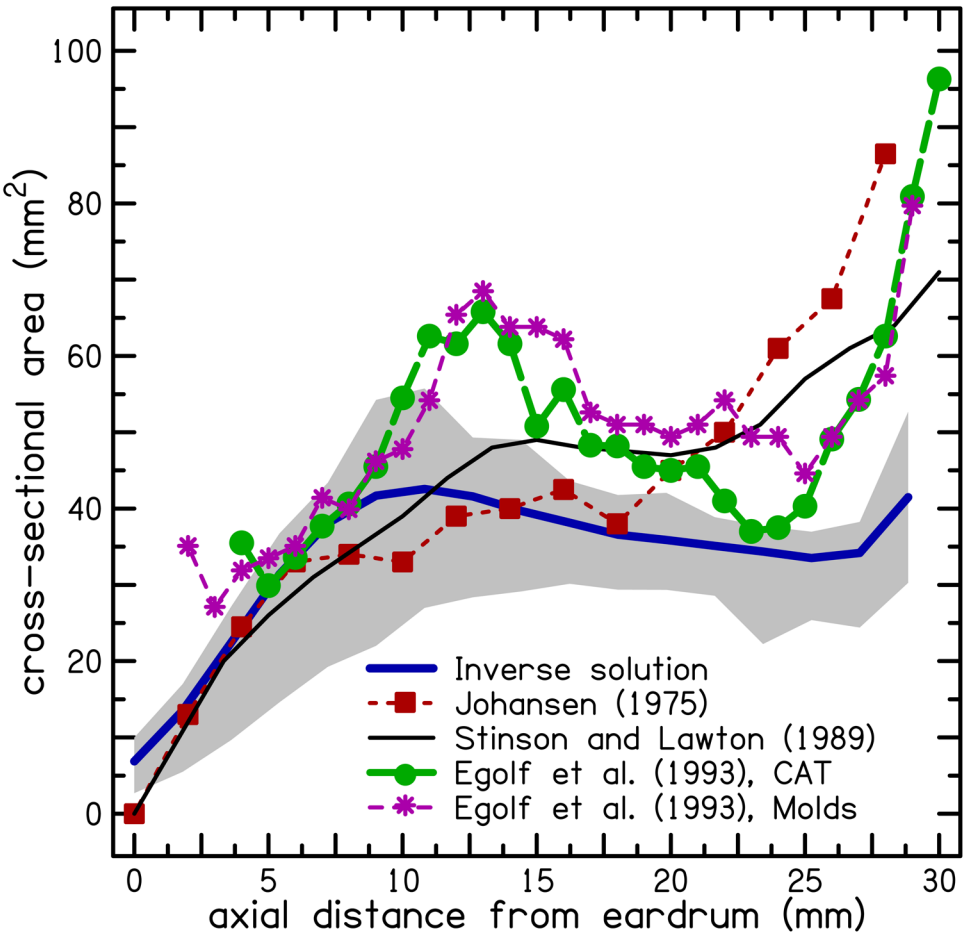

Figure 5.
Mean ear-canal area function obtained from inverse solution. Shaded region indicates data between the 25th and 75th percentiles. The location of the eardrum is $x = 0$. Comparison is made to data from Johansen (1975), Stinson and Lawton (1989) and Egolf *et al.* (1993). The mean ear-canal area function of the current study is similar to the area functions reported by the earlier studies. Reprinted with permission from Rasetshwane D.M., & Neely, S.T., Journal of the Acoustical Society of America, 130, 3873–3881. Copyright (2011), Acoustical Society of America.

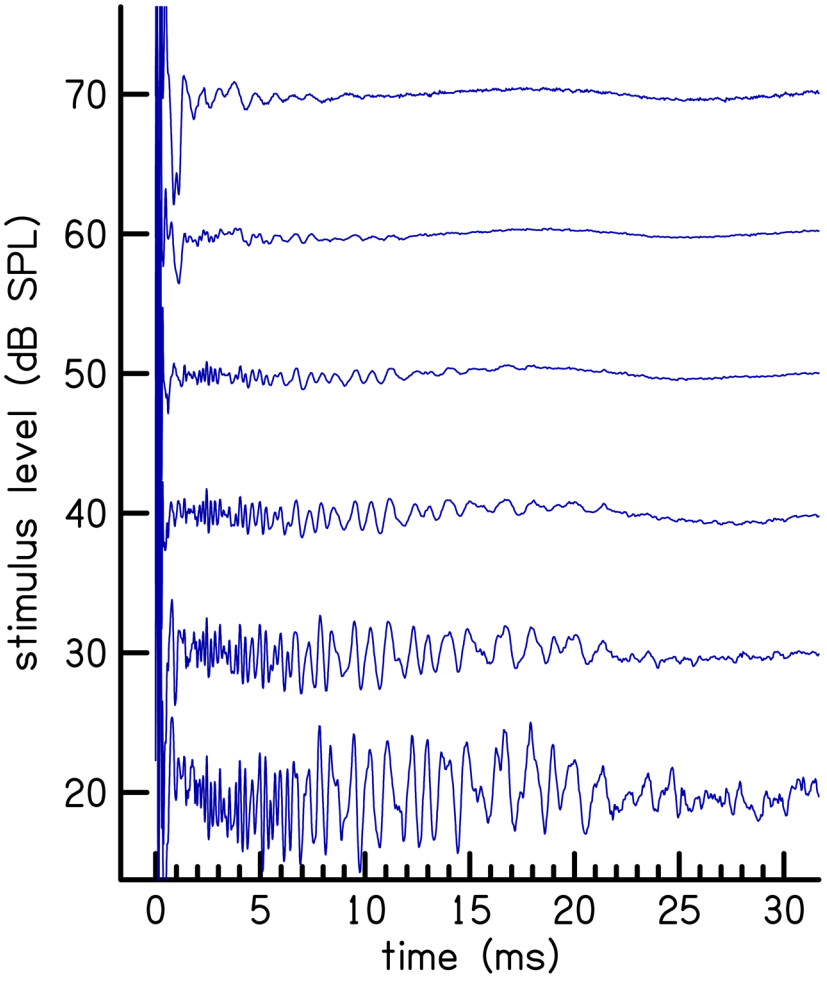

Figure 6.

Time-domain cochlear reflectance after the subtraction procedure and before the time-frequency analysis. The label on the ordinate axis indicates the stimulus level used to elicit each reflectance waveform. High frequency content temporally precedes low frequency content in the time-domain CR. The activity below $t = 1$ ms is middle-ear activity that was not removed by the subtraction procedure. Reprinted with permission from Rasetshwane D.M., & Neely, S. T., Journal of the Acoustical Society of America, 13, 591–607. Copyright (2012), Acoustical Society of America.

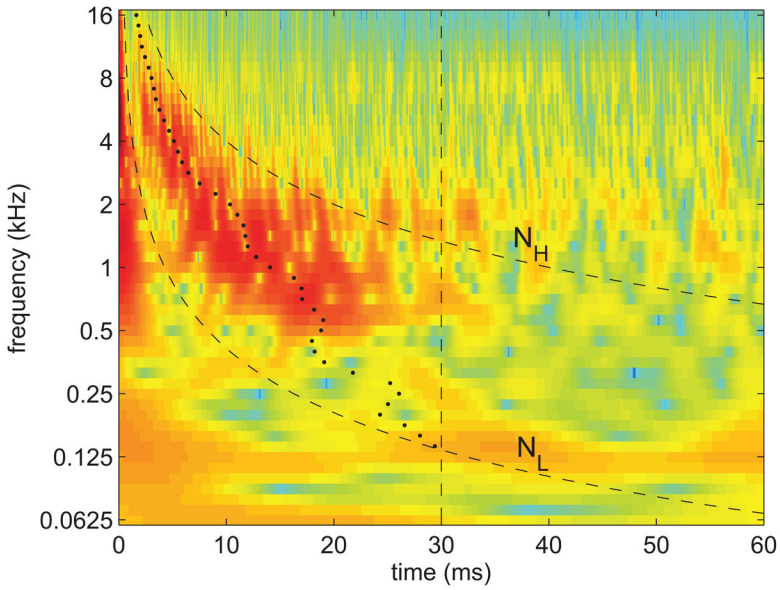

Figure 7.

Time-frequency analysis of CR using the gammatone spectrogram. The region of high energy of the gammatone spectrogram enclosed by functions N_L and N_H includes most of the exponential decaying energy of CR. The region below N_L includes residual middle ear and measurement system activity that was not removed by the subtraction procedure. The activity beyond $t = 30$ (indicated with vertical dashed line) is due to re-reflection of the traveling wave. The dots are estimates of the group delay. Reprinted with permission from Rasetshwane D.M., & Neely, S.T., Journal of the Acoustical Society of America, 13, 591–607. Copyright (2012), Acoustical Society of America.